

## Patterned growth of single-walled carbon nanotubes on full 4-inch wafers

Nathan R. Franklin, Yiming Li, Robert J. Chen, Ali Javey, and Hongjie Dai<sup>a)</sup>  
*Department of Chemistry, Stanford University, Stanford, California 94305*

(Received 20 September 2001; accepted for publication 19 October 2001)

Patterned growth of single-walled carbon nanotubes (SWNTs) is achieved on full 4-in. SiO<sub>2</sub>/Si wafers. Catalytic islands with high uniformity over the entire wafer are obtained by a deep ultraviolet photolithography technique. Growth by chemical vapor deposition of methane is found to be very sensitive to the amount of H<sub>2</sub> co-flow. Understanding of the chemistry enables the growth of high quality SWNTs from massive arrays (10<sup>7</sup>–10<sup>8</sup>) of well-defined surface sites. The scale up in patterned nanotube growth shall pave the way to large-scale molecular wire devices. © 2001 American Institute of Physics. [DOI: 10.1063/1.1429294]

Single-walled carbon nanotubes (SWNTs) are ideal quantum systems for exploring basic science in one dimension.<sup>1</sup> These molecular-scale wires, derived by bottom-up chemical synthesis approaches, are also promising as core components or interconnecting wires for future electronics. Indeed, rich quantum phenomena have been revealed with SWNTs<sup>2–5</sup> and functional electronic devices have been built such as transistors,<sup>3,4</sup> chemical sensors,<sup>6,7</sup> and memory devices.<sup>8</sup> From both fundamental and practical point of views, it is desirable to assemble nanotubes into ordered structures on large surfaces for addressable and integrated devices. Not only should the assembly methods be able to place nanotubes at specific locations with desired orientations, the methods must be scalable to large areas.

Patterned growth of carbon nanotubes [e.g., by chemical vapor deposition (CVD)] represents an assembly approach to place and orient nanotubes at a stage as early as when they are synthesized.<sup>9,10</sup> Catalyst patterning defines the locations from which nanotubes originate,<sup>11–14</sup> and van der Waals self-assembly<sup>12,15,16</sup> or external fields<sup>17</sup> determine their orientations. While this approach has been effective in yielding SWNTs on small substrates for basic studies and device demonstrations, little is known about the scalability of surface catalytic patterning and the chemistry needed for growing nanotubes in large reactors.

Here we report the patterned growth of SWNTs on full 4-in. SiO<sub>2</sub>/Si wafers. Wafer-scale catalytic patterning is achieved by deep ultraviolet (DUV) photolithography and spin casting. Catalyst islands with remarkable uniformity over the entire wafer are obtained. CVD of CH<sub>4</sub> (Refs. 11 and 18) at elevated temperatures is found to be ultrasensitive to the amount of H<sub>2</sub> co-flow, undergoing pyrolysis, growth, and inactive reaction-regimes with increased H<sub>2</sub> addition. Understanding of the chemistry enables the growth of high quality SWNTs from massive arrays (10<sup>7</sup>–10<sup>8</sup>) of well-defined surface sites on full 4-in. wafers.

A SiO<sub>2</sub>/Si wafer was first coated with 300 nm thick of poly(methylmethacrylate) (PMMA) and exposed through a quartz mask to DUV under a Karl–Suss MA-6 photolithography system by using a home-assembled optical setup (light source: Oriel 200 W Hg Arc Lamp with Sun Lens beam

diffuser by Spectral Energy). Developing the exposed regions resulted in large arrays of wells in the PMMA. A suspension of Al<sub>2</sub>O<sub>3</sub> supported Fe/Mo catalyst in methanol<sup>11</sup> was spun onto the wafer at a low speed of 250 revolutions-per-minute followed by baking at 160 °C for 5 min. The wafer was then immersed in dichloroethane to lift off the PMMA, which afforded remarkably uniform catalyst arrays over the entire 4-in. wafer [Fig. 1(a)]. The catalyst islands vary in size down to 1 μm, limited by the mask resolution. We employed DUV and PMMA resist for catalytic patterning since PMMA was not dissolved by methanol in the catalyst suspension. Further, lift off of PMMA afforded a clean and smooth wafer surface with no PMMA residue left on the surface. With commonly used photoresists however, an undesired “scum” residue layer with roughness on the order of 10 nm was always left on the surface upon lift off.

CVD was carried out in at 900 °C for 7 min with the wafer placed in a 4-in.-diameter (48-in. long heating zone, Lindberg Blue) quartz tube furnace [Fig. 1(b)]. Pure CH<sub>4</sub> (99.999%) at a fixed flow rate of 1500 ml/min (1080 ml/min when the gas correction factor of 0.72 for methane is taken into account) was used for carbon feedstock. To investigate the growth conditions, H<sub>2</sub> was co-flow at a rate in the range of 50 to 150 ml/min.

Strikingly different CVD growth results are obtained

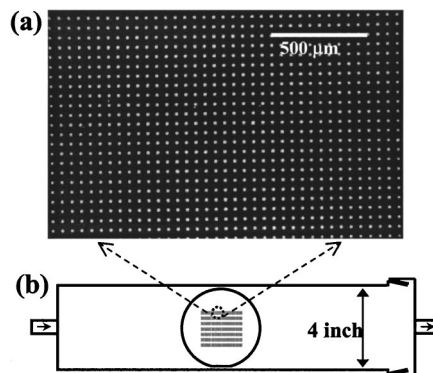


FIG. 1. (a) Optical image of an array of catalyst islands (side length 10 μm) patterned on a wafer using DUV lithography. (b) Diagram of the quartz tube reactor used for growth of nanotubes. Gases are introduced on the left-hand side and flow on the wafer placed in the center of the reactor. Exhaust leaves through the port on the right-hand side. The right-hand side cap of the tube is removable for wafer transfer.

<sup>a)</sup>Electronic mail: hdai1@stanford.edu

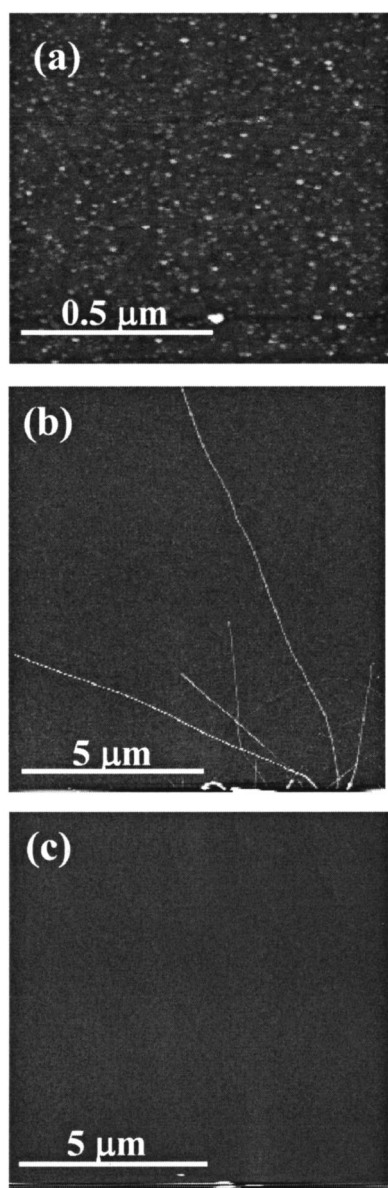


FIG. 2. AFM images of wafer surfaces near catalyst islands. (a) A rough surface with a significant amount of amorphous carbon deposits formed in the pyrolysis regime under a  $H_2$  co-flow of 50 ml/min. (b) A clean surface and good yield of SWNTs grown from a catalyst island (at the bottom of the image, not shown) in the growth regime under a  $H_2$  co-flow of 125 ml/min. (c) A clean surface but zero yield of SWNTs in the inactive regime with 150 ml/min  $H_2$  co-flow.

when varying the amount of  $H_2$  co-flow. The best condition for yielding high quality SWNT is with 125 ml/min  $H_2$  co-flow. Figure 2(b) is an atomic force microscopy (AFM) image showing the typical results of SWNTs grown from patterned catalyst islands. Large numbers of SWNTs are observed near every island. Typically, several tubes emanate from the islands, extending to  $\sim 10 \mu\text{m}$  lengths. These long SWNTs are desired for device integrations. Growth results from catalyst islands across the entire 4-in. wafer are very consistent and uniform. Importantly, the  $\text{SiO}_2$ -wafer surface is clean without amorphous carbon deposits, indicating negligible  $\text{CH}_4$  self-pyrolysis in the gas phase. We define the 1500 ml/min  $\text{CH}_4$  and  $\sim 125$  ml/min  $H_2$  condition as in a desired “growth-regime” (Fig. 3).

A “pyrolysis-regime” was identified when  $H_2$  co-flow was lowered to  $\sim 50$  ml/min [Figs. 2(a) and 3]. Few SWNTs

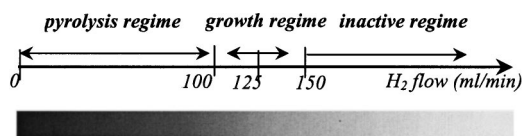


FIG. 3. Schematic presentation of three regimes of CVD growth conditions in a 4-in. system at  $900^\circ\text{C}$  under a 1500 ml/min flow of  $\text{CH}_4$ . Darkness of the bar represents the amount of active carbon species in the three regimes.

were grown from catalyst islands, with AFM revealing the  $\text{SiO}_2$ -wafer surface covered by amorphous carbon deposits [Fig. 2(a)]. Worse was the observation of oily coating on the reactor wall by higher hydrocarbons generated during vigorous  $\text{CH}_4$  pyrolysis. In contrast, an ‘inactive-regime’ was encountered when  $H_2$  flow increased above  $\sim 150$  ml/min [Figs. 2(c) and 3]. Clean wafer surface and reactor wall were seen but the yield of SWNTs from the catalytic islands was low (Fig. 3).

Thus, we have identified three regimes of  $\text{CH}_4$ -CVD conditions parameterized by  $H_2$  concentration under a constant  $\text{CH}_4$  flow in the 4-in.-CVD system (Fig. 3). The chemical reactivity of  $\text{CH}_4$  is sensitive to  $H_2$ , a well-known phenomenon in hydrocarbon pyrolysis chemistry.<sup>19</sup>  $H_2$  serves to decrease the rate of  $\text{CH}_4$  decomposition by hydrogenating reactive carbon species.<sup>19</sup> Its presence slows down the  $\text{CH}_4$  decomposition since  $H_2$  is a product of the reaction. Nevertheless, our current finding of high sensitivity of SWNT growth to  $H_2$  in  $\text{CH}_4$  CVD is striking considering the small variations in  $H_2$  concentrations that distinguish the three regimes (Fig. 3). In the pyrolysis regime ( $H_2 < \sim 50$  ml/min),  $\text{CH}_4$  decomposition is vigorous without effective  $H_2$  inhibition. Amorphous carbon generation causes catalyst poisoning and low SWNT yield. In the inactive-regime ( $H_2 > 150$  ml/min), the concentration of  $H_2$  lowers the  $\text{CH}_4$  reactivity below a level needed for  $\text{CH}_4$  as an efficient carbon feedstock to the catalyst. In the growth regime ( $H_2 \sim 125$  ml/min), the concentration of  $H_2$  allows a good balance to prevent undesired amorphous carbon formation and maintain the  $\text{CH}_4$  reactivity, leading to excellent results in catalytic SWNT growth. It should be noted that the growth conditions and results are also very sensitive to impurities in the methane gas and potential metal contaminations in the CVD quartz chamber. For consistent results, it is important to use ultra-high purity methane as in the present work and avoid metal contamination of the system (due to deposition of vaporized metal species, e.g., Mo, onto the wall of the quartz chamber).

The aforementioned chemistry is essential to identifying highly reproducible and controllable growth conditions, and key to our patterned SWNT growth on full 4-in. wafers. More importantly, the understanding is general and applicable to predicting growth conditions for different temperatures and  $\text{CH}_4$  flow rates, and can be extended to CVD growth for multiwalled nanotubes.<sup>20</sup> For instance, at  $950^\circ\text{C}$ , a growth regime for SWNT is identified with 1500 ml/min  $\text{CH}_4$  flow and 200 ml/min  $H_2$  co-flow. This condition is found when increasing the  $H_2$  concentration just beyond the pyrolysis regime. The reactivity of methane is higher at a more elevated temperature ( $950^\circ\text{C}$  vs  $900^\circ\text{C}$ ), thus, a higher concentration of  $H_2$  (200 vs 125 ml/min) is required to inhibit  $\text{CH}_4$  decomposition and bring the system into the nanotube growth regime.

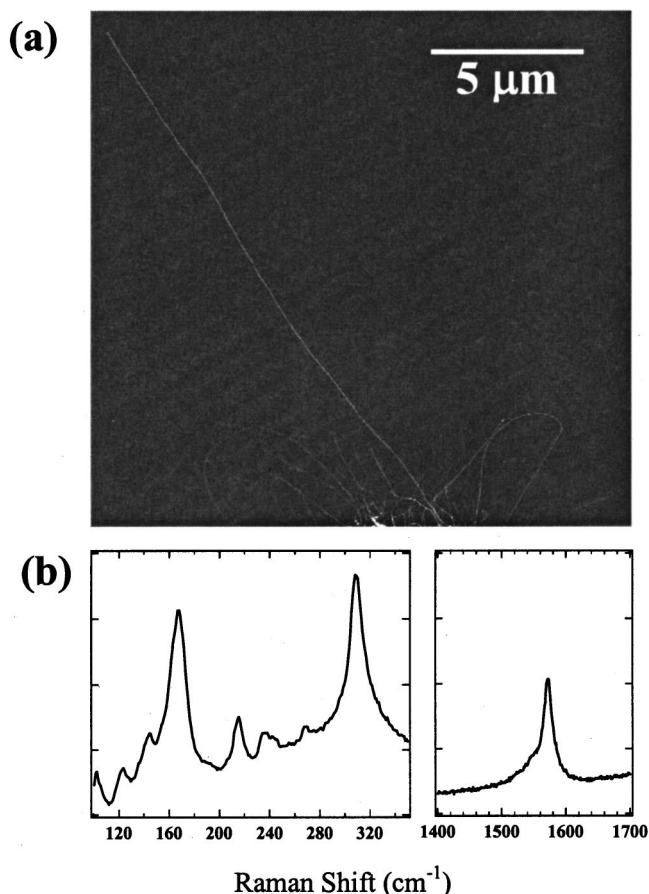


FIG. 4. (a) AFM image of nanotubes grown from a catalyst island (at the bottom of the image, not shown) on a 4-in. wafer. (b) Raman spectra of carbon nanotubes growing off of a catalyst island.

The patterned growth of SWNTs on full 4-in. wafers presented here is highly reproducible and controllable. Importantly, AFM characterization reveals no drastic variations in the yield of nanotubes from catalytic islands across the wafer surface with typically 1 to 3 long SWNTs emanating from each island [Figs. 4(a) and 2(b)]. The SWNTs are also characterized by resonant micro-Raman spectroscopy<sup>21</sup> (Renishaw, 785 nm laser) using a 1  $\mu\text{m}$  laser beam focused a few microns away from catalyst islands. The spectra show very typical SWNT axial vibration modes around 1590  $\text{cm}^{-1}$  and radial breathing modes (RBM) around 120–320  $\text{cm}^{-1}$  [Fig. 4(b)], confirming that high quality SWNTs (diameters  $d \sim 1\text{--}3$  nm, RBM Raman shift<sup>21</sup>  $\sim 1/d$ ) are synthesized from catalytic patterns.

The scale up of patterned growth allows for high quality SWNTs readily integrated into electrical circuits at the wafer scale. This is done by carrying out a wafer-scale photolithog-

raphy step for metal contacts of the nanotubes around each catalytic island after CVD synthesis. Detailed results of electrical transport properties and devices with the nanotube arrays will be presented elsewhere.

In conclusion, we have succeeded in patterned growth of massive arrays of SWNTs at the full-wafer scale. The chemistry of  $\text{CH}_4$  CVD is found to be sensitive to the concentration of  $\text{H}_2$ , leading to three regimes of growth conditions. This very understanding has enabled our synthesis scalability. We believe that the understanding could also be useful for CVD type of synthesis of other nanomaterials. The results here shall pave the way for patterned growth at the individual catalytic nanoparticle<sup>22</sup> level, nanotube orientation control and device integration in a scalable fashion for future nanoelectronics.

This work is supported by DARPA, the MARCO MSD Focus Center, NSF, SRC/Motorola, a Packard Fellowship, a Sloan Fellowship, and a Terman Fellowship.

<sup>1</sup>M. S. Dresselhaus, G. Dresselhaus, and P. C. Eklund, *Science of Fullerenes and Carbon Nanotubes* (Academic, San Diego, 1996).

<sup>2</sup>C. Dekker, *Phys. Today* **52**, 22 (1999).

<sup>3</sup>P. L. McEuen, *Phys. World* **13**, 31 (2000).

<sup>4</sup>W. Liang, M. Bockrath, D. Bozovic, J. Hafner, M. Tinkham, and H. Park, *Nature (London)* **411**, 665 (2001).

<sup>5</sup>J. Kong, E. Yenilmez, T. W. Tombler, W. Kim, L. Liu, C. S. Jayanthi, S. Y. Wu, R. B. Laughlin, and H. Dai, *Phys. Rev. Lett.* **87**, 106801 (2001).

<sup>6</sup>J. Kong, N. Franklin, C. Zhou, M. Chapline, S. Peng, K. Cho, and H. Dai, *Science* **287**, 622 (2000).

<sup>7</sup>P. G. Collins, K. Bradley, M. Ishigami, and A. Zettl, *Science* **287**, 1801 (2000).

<sup>8</sup>T. Rueckes, K. Kim, E. Joselevich, G. Y. Tseng, C. L. Cheung, and C. M. Lieber, *Science* **289**, 94 (2000).

<sup>9</sup>H. Dai, *Phys. World* **13**, 43 (2000).

<sup>10</sup>H. Dai, in *Carbon Nanotubes*, edited by M. S. Dresselhaus, G. Dresselhaus, and P. Avouris (Springer, Berlin, 2001), Vol. 80, p. 29.

<sup>11</sup>J. Kong, H. Soh, A. Cassell, C. F. Quate, and H. Dai, *Nature (London)* **395**, 878 (1998).

<sup>12</sup>S. Fan, M. Chapline, N. Franklin, T. Tombler, A. Cassell, and H. Dai, *Science* **283**, 512 (1999).

<sup>13</sup>Y. Yang, S. Huang, H. He, A. Mau, and L. Dai, *J. Am. Chem. Soc.* **121**, 10832 (1999).

<sup>14</sup>G. Gu, G. Philipp, X. Wu, M. Burghard, A. Bittner, and S. Roth, *Adv. Func. Mater.* **11**, 295 (2001).

<sup>15</sup>A. Cassell, N. Franklin, T. Tombler, E. Chan, J. Han, and H. Dai, *J. Am. Chem. Soc.* **121**, 7975 (1999).

<sup>16</sup>N. Franklin and H. Dai, *Adv. Mater.* **12**, 890 (2000).

<sup>17</sup>Y. Zhang, A. Chan, J. Cao, Q. Wang, W. Kim, Y. Li, N. Morris, E. Yenilmez, J. Kong, and H. Dai (unpublished).

<sup>18</sup>M. Su, B. Zheng, and J. Liu, *Chem. Phys. Lett.* **322**, 321 (2000).

<sup>19</sup>A. Dean, *J. Phys. Chem.* **94**, 1432 (1990).

<sup>20</sup>D. Wang, P. Qi, and H. Dai (unpublished result).

<sup>21</sup>A. Jorio, R. Saito, J. H. Hafner, C. M. Lieber, M. Hunter, T. McClure, G. Dresselhaus, and M. S. Dresselhaus, *Phys. Rev. Lett.* **86**, 1118 (2001).

<sup>22</sup>Y. Li, J. Liu, Y. Wang, and Z. L. Wang, *Chem. Mater.* **13**, 1008 (2001).